

Defect Induced Band Gap narrowing of Zinc Oxide Nanoparticles using Li^+ , Na^+ and K^+ Metal Ions as a Dopant

Tizita Girma, Khalid Siraj* and Alemayehu Yifru

Department of Chemistry, College of Natural Sciences, University of Jimma, P.O. Box 378, Jimma, Ethiopia.

ARTICLE INFO

Article history:

Received: 28 December 2015;

Received in revised form:

28 January 2016;

Accepted: 2 February 2016;

Keywords

ZnO Nanoparticles,
Band Gap Energy,
Alkali Metals,
Doping,
UV-Vis Spectroscopy.

ABSTRACT

This paper mainly explain the lowering of band gap energy of synthesized ZnO nanoparticles (3.263eV) than their bulk counterparts (3.37 eV), which indicate the high conductivity than the bulk ZnO powder. $\text{Zn}_{1-x}\text{Li}_x\text{O}$, $\text{Zn}_{1-x}\text{Na}_x\text{O}$ and $\text{Zn}_{1-x}\text{K}_x\text{O}$ (where $x=0.005, 0.01, 0.015$ and 0.02 M for all dopants) doped ZnO nanoparticles and their solution was then characterized by UV-vis spectrophotometer. All concentration of Li^+ doped ZnO nanoparticles was more narrowing the band gap of the undoped ZnO nanoparticles than Na^+ and K^+ doped ZnO nanoparticles. Both the size and concentration of dopants were affecting the band gap energy of ZnO nanoparticles. As the concentration and ionic radii of the dopants increases the optical band gap energy was also increasing. So the highest band gap energy was obtained by 0.015 and 0.02M K^+ doped ZnO nanoparticles.

© 2016 Elixir all rights reserved.

Introduction

ZnO is regarded as an ideal alternative material for ITO (Indium Thin Oxide) because of its lower cost and easier etchability [1]. The native doping of the semiconductor due to oxygen vacancies or Zinc interstitials is n-type [2]. In comparison with Si semiconductor, which is widely used in the display industry, metal oxide semiconductors show high electrical performance as well as unique properties, including good transparency, high electron mobility, wide bandgap and strong room-temperature luminescence. Those properties are used in emerging applications for transparent electrodes in liquid crystal displays; in energy saving or heat protecting windows and in electronics as thin film transistors and light-emitting diodes. The band gap is the major factor determining the electrical conductivity of a solid, Fig. 1.

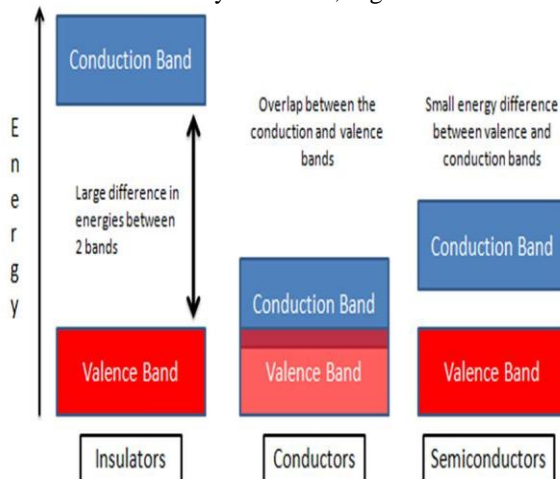


Figure 1. The differences between band gaps of different Materials

It is well known that the changes in band gap energies could occur when impurities were added to a wide gap semiconductor and there is a higher degree of atomic homogeneity [3]. The group IA elements are used as doping materials to improve and tune the optical and band gap energy of ZnO [4]. However, being smaller in atomic radii, group IA elements prefer to occupy the interstitial sites, rather than substitutional sites and therefore, act mainly as donors [5].

It is very difficult to obtain P-type doping in wide-band-gap semiconductors such as GaN, ZnO and ZnSe. The difficulties to form shallow acceptor level arise mainly from (i) low solubility of the dopant in the host material, (ii) compensation of dopants by low energy native defects, like, Zn interstitials or oxygen vacancies or background impurities and (iii) deep impurity level.

To overcome those difficulties, one would expect that the P-type doping in ZnO may be possible by substituting either group IA elements like, Li, Na, and K for Zn sites or group-V elements as N, P, and as for oxygen sites [6].

In the ZnO-based metal oxide semiconductors TFTs, UV-visible spectroscopy analysis can be simply used as analysis tool because of their unique optical property like transparency [7].

Materials and Methods

Chemicals

Zinc Acetate dihydrate ($\text{Zn}(\text{CH}_3\text{COOH})_2 \cdot 2\text{H}_2\text{O}$) (Finken, 98%), Sodium hydroxide (NaOH) (Finken, 97%), Lithium Nitrate (LiNO_3) (Nice, 97%), Sodium Nitrate (NaNO_3) (Nice, 97%), Potassium Nitrate (KNO_3) (Nice, 97%), Ethanol (Hylux, 98%), Deionized water and Distilled water.

Instrument and materials

Analytical balance, Oven, Volumetric flask, Measuring cylinder, Ultrasonic wave irradiation, Quartz cuvette, Hot plate and JENWAY 6705 UV-visible spectrophotometer

Procedures

Preparation of ZnO nanoparticles

50 mL of aqueous solution of 0.2 M Zinc acetate dehydrate ($\text{Zn}(\text{CH}_3\text{COOH})_2 \cdot 2\text{H}_2\text{O}$) was added to 10 mL of aqueous solution of 0.2 M Sodium hydroxide (NaOH) and subjected to ultrasonic wave irradiation for 2 h. The obtained white precipitate was filtered and washed with Deionized water and Ethanol and dried in an oven at 60°C for 2 h. Then sample was calcined (heated) at 400°C for 2 h to evaporate the solvent and to remove organic residuals. The solution was carried out using JENWAY 6705 UV-visible spectrophotometer.

Preparation of Sodium, lithium and potassium ions doped ZnO nanoparticles

0.015 M of LiNO_3 , NaNO_3 and KNO_3 was each prepared in 50 mL of deionized water and the serial dilution of 0.010 M and 0.005 M was prepared in 10 ml of deionized water for each dopants. 10 mL of each concentration was doped to ZnO nanoparticles, then each solution of doped ZnO nanoparticles was calcined at 400°C for 2 h and then each powder was prepared in 100 ml of deionized water. Absorbance measurement was carried out to characterize doped ZnO by UV-Vis spectroscopy to determine their band gap energy from Tauc's relationship by extrapolating straight line along the

Results and Discussion

Absorption spectrum

A spectrophotometer was used to measure the amount of light absorbed by a substance. An absorption spectrum was the plot of the absorbance versus the wavelength of the incident light.

Characterization of ZnO nanoparticles

UV-visible spectrophotometer is widely used techniques to examine the optical properties of nanosized particles. In this work, deionized water was used as a blank for adjusting the instrument. Then the absorbance of the ZnO nanoparticles solution was measured using a quartz tube. The UV-vis absorption spectra of the samples were recorded in the wavelength range of 260 to 500 nm. Figure 2, illustrates the UV-vis spectrum of ZnO nanoparticles

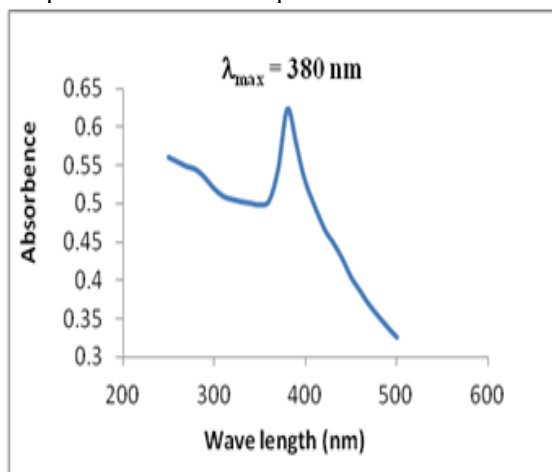


Figure 2. UV-Vis absorption spectrum of ZnO nanoparticles

As can be seen, from the above figure, ZnO nanoparticles exhibited maximum absorption of 380 nm, indicating red shift when compared with the bulk powder of ZnO, (absorption

maxima, 368 nm). This can be assigned to the intrinsic band gap absorption of ZnO due to the electron transitions from the valence band to the conduction band [8].

Tauc's law plot of ZnO nanoparticles

This plot was used to determine the band gap energy by extrapolating straight line to the x-axis. Fig 3, shows Tauc's law plot of ZnO nanoparticles, Which was constructed as $(\alpha h\nu)^2$ as a function of photon energy ($h\nu$) of the nanoparticles

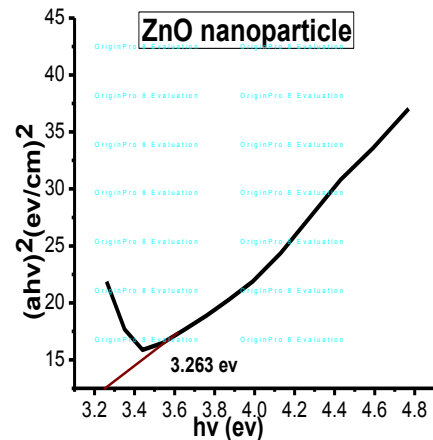


Figure 3. Plots of $(\alpha h\nu)^2$ versus photon energy ($h\nu$) of ZnO nanoparticles

The optical band gap energy of the nanoparticles was determined by applying the Tauc's relationship [9].

$$(\alpha h\nu) = c(h\nu - E_g)^{1/2}$$

Where;

α is the optical absorption coefficient ($\alpha = 2.303A/t$ here, A is the absorbance and t is the thickness of the cuvette), E_g is the band gap energy, $h\nu$ is the energy of the radiation (photon energy), c is a constant that is independent of the photon energy. As can be seen from the Fig. 3 the band gap energy of the prepared ZnO nanoparticles was ≈ 3.263 eV, which is narrower than that of the bulk (3.37 eV). Nanoparticles show lattice contraction due to high attractive electrostatic interaction between Zn^{2+} and O^{2-} ions.

The size of the particle was obtained from the absorbance spectra by calculating using formula, which was derived from effective mass model. As compared to bulk ZnO powder, the absorption edge of prepared ZnO nanoparticles was systematically shifted to higher wavelength (red shifted) or lower band gap energy with increasing size of the nanoparticles. This pronounced and systematic shift in the absorption edge was due to the quantum size effect [10].

The following equation was derived using the effective mass model to determine the particle size (radius) as a function of peak absorbance wavelength (λ_p) for the monodispersed ZnO nanoparticles

$$r_{(nm)} = \frac{-0.3049 + \sqrt{-26.23012 + \frac{10240.72}{\lambda_p}}}{-6.3829 + \frac{2483.2}{\lambda_p}}$$

$$E = E_g^{bulk} + \frac{h^2 \pi^2}{2\mu r^2} - 1.8 \frac{e^2}{\epsilon r} - 0.248 E_{RY}^*$$

Where

$$\frac{1}{\mu} = \frac{1}{m_e^*} + \frac{1}{m_h^*}; E_{RY}^* \text{ in } m^{-1} = \frac{m_e e^4}{8\epsilon_0^2 h^3 c}; E_{RY}^* \text{ in } eV = E_{RY}^* hc$$

where,

E_{RY}^* is the effective Rydberg energy,

E_g^{bulk} is the bulk band gap energy (≈ 3.37 eV),

μ is the reduced mass,

r is sphere radius (particle size),

h is Plank's constant (6.626×10^{-34} m²kg/s),

m_e^* is the electron effective mass (0.26),

m_h^* is the hole effective mass (0.59).

In this work, the prepared ZnO nanoparticles have a particle size of 3.6 nm, indicating no expectation for band gap enlargement. It has been referred that the band gap enlargement is not expected for ZnO nanoparticles size of less than 4 nm [11]. e is the charge on the electron (1.602×10^{-19} C), ϵ_0 is the permittivity of free space (8.85×10^{-12} F/m) and ϵ is the relative permittivity (8.5). On effective mass formula, the first term on the right hand side represents the band gap of bulk materials, The second additive term of the equation represents the additional energy due to quantum confinement having $1/r^2$ dependence on band gap energy and the third subtractive term stands for the columbic interaction energy of exciton having $1/r$ dependence on band gap energy, often neglected due to high dielectric (relative permittivity) constant of the material [12].

Optical properties of different concentration of Li⁺, Na⁺ and K⁺ doped ZnO

The magnitude of bandgap shift due to moderate or heavy doping level was determined by two competing mechanisms; band gap narrowing (BGN) which was a consequence of many-body effects on the conduction and valence bands and the bandgap widening (BGW) which was referred to the well known Burstein–Moss effect.

Characterization of Li⁺, Na⁺ and K⁺ doped ZnO nanoparticles

The maximum absorption peak of each concentration was determined from their corresponding spectra. The UV–Visible absorption spectra of different concentration Li⁺, Na⁺, K⁺ doped and undoped ZnO nanoparticles was shown in figure, 4, table 1. In all cases, the obtained results demonstrated that the absorption maxima's of nanoparticles were changed with the change of the type of the dopants and as well as their concentrations. The absorption maxima present the wavelength at which take place between valence and conduction bands [13]. The dopant that have larger wavelength was red shifted, with decreasing the band gap energy of undoped ZnO nanoparticles. From all those dopants 0.015 M Li⁺ doped ZnO nanoparticles have highest wavelength and narrow band gap. 0.02 M K⁺ doped ZnO nanoparticles have lowest wavelength than others that means it was blue shifted due to its larger ionic size and low electronegativity.

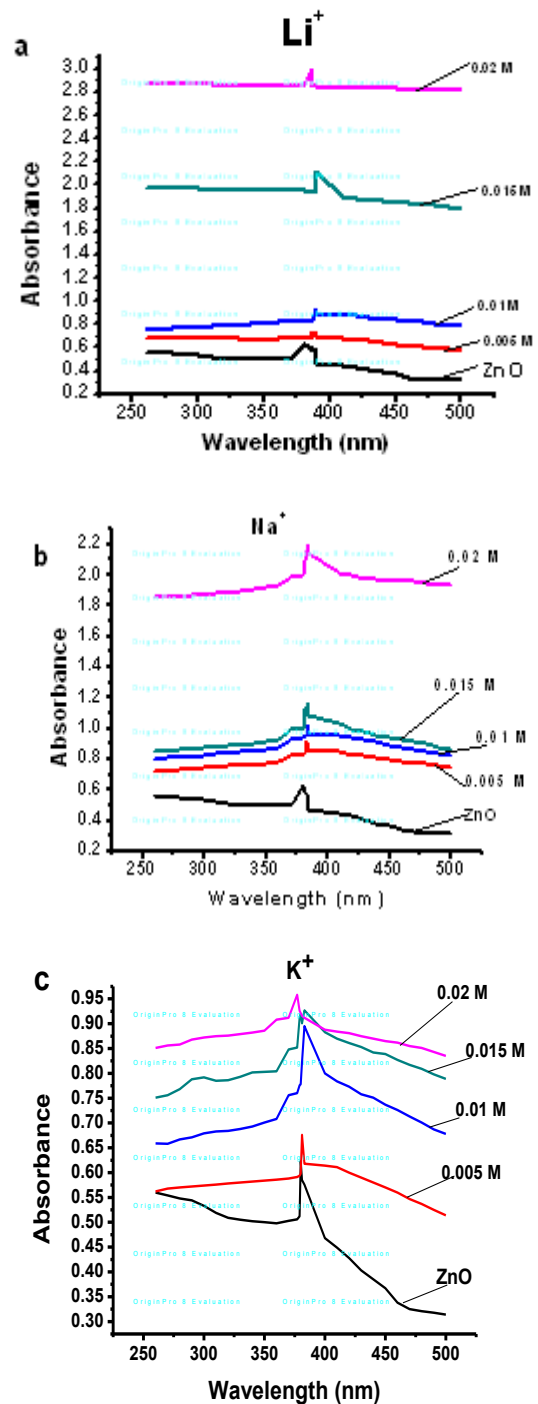


Figure 4. The UV–Visible absorption spectra of a) Li⁺, b) Na⁺ and c) K⁺ doped and undoped ZnO nanoparticles

Table 1. Maximum absorption peaks of different concentration doped ZnO nanoparticles

Dopants	λ_{max} (nm)				Undoped ZnO $\lambda_{max} = 380$ nm
	0.005 M	0.01 M	0.015 M	0.02 M	
Li ⁺	387	389	390	386	
Na ⁺	383	385	384	381	
K ⁺	381	383	379	377	

Effect of doping on band gap energy of ZnO nanoparticles

Plots of $(\alpha h\nu)^2$ vs $h\nu$ for undoped ZnO nanoparticles and 0.005, 0.01, 0.015 and 0.02 M of Li⁺, Na⁺ and K⁺ doped ZnO nanoparticles was shown in figure, 5, Table 2. The obtained results demonstrated that the band gap energy of Li⁺ doped ZnO nanoparticles decrease with increasing concentration of the dopant Li⁺. This might be attributed to the increase of oxygen vacancies, resulting from the introduction of Li⁺ at Zn²⁺ sites [14].

Table 2. The band gap energy of undoped and different concentrations of Li⁺, Na⁺ and K⁺ doped ZnO nanoparticles

Metal ion	Ionic Size (nm)	Band gap (eV)			
		0.005M	0.01M	0.015M	0.02
Li ⁺	0.068	3.198	3.195	3.179	3.212
Na ⁺	0.097	3.237	3.22	3.228	3.268
K ⁺	0.133	3.268	3.237	3.271	3.289
Zn ²⁺	0.074	-	-	-	-

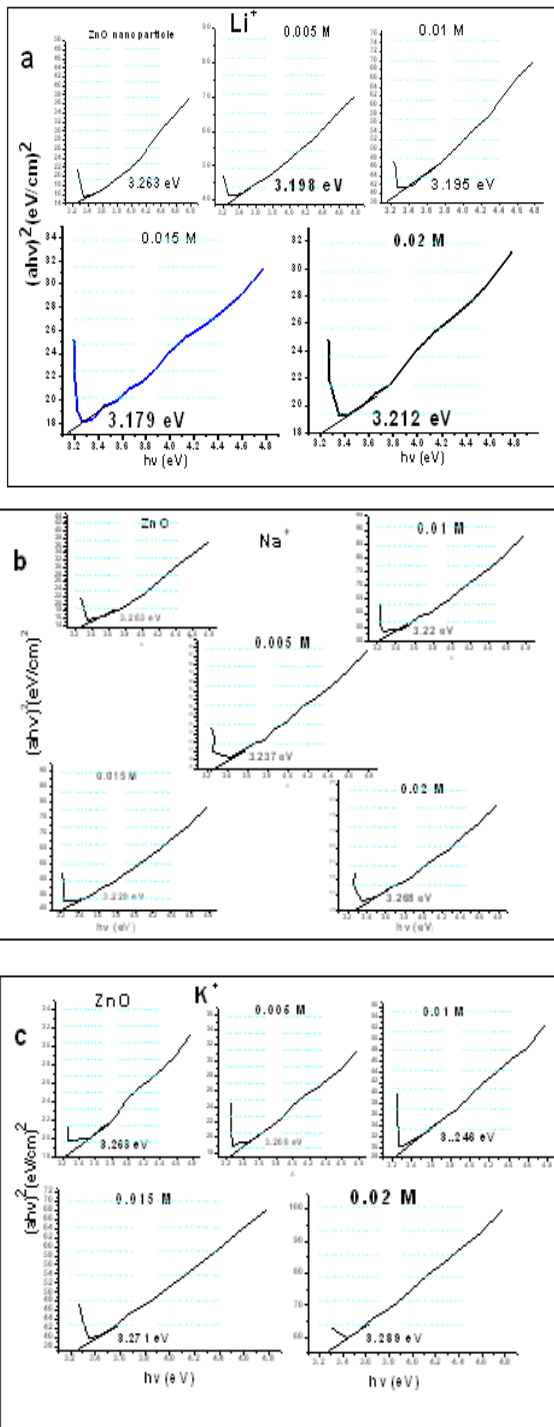


Figure 5. Plots of $(\alpha hv)^2$ vs hv for undoped ZnO Nanoparticles and different concentrations of a) Li⁺, b) Na⁺ and c) K⁺ doped ZnO nanoparticles

For all different concentrations the band gap energy indicating minimum band gap energy for the smaller ion, Li⁺ and the highest for the largest ion, K⁺, among the studied dopant, alkali metals. So Na⁺ and K⁺ due to doped ZnO

nanoparticles its smallest ionic radii and highest electronegativity of Na and K[15], it attracts bonding electrons strongly than others, Na⁺ and K⁺, its lower ionic radii of Li⁺ than Zn²⁺. Moreover, its higher electronegativity then demonstrated the highest change in the conductivity of Li⁺ doped ZnO nanoparticles.

From all dopants 0.015 and 0.02 M K⁺ doped ZnO nanoparticles the band gap energy of undoped ZnO nanoparticles increases from 3.263 to 3.271 and 3.289eV respectively. The larger size as well as concentration of the dopant increases the band gap energy, due to the Fermi level to push to conduction band above edge and such doping induced band-filling called as Burstein-Moss shift. So the contribution of K⁺ ions on interstitial sites of Zn²⁺ ion determines the widening of the band gap caused by an increase in carrier concentration [15].

The difference in band gap of undoped and doped ZnO nanoparticles was observed due to the incorporation of dopants in ZnO lattice. As the size and concentration of dopant increases, Oxygen vacancy decreases, because the opportunity of freely moving electrons from valence band to conduction band decreases. That means the introduction of larger size dopant enhances the crystallinity of ZnO nanoparticles, and hence band gap energy increases. Undoped ZnO nanoparticles have conductivity by electrons, but when it is doped with different concentration of Li⁺, Na⁺ and K⁺ its conductivity is varied.

Red-shift of fundamental absorption edge was observed when the band gap energy was narrowed in comparison to undoped ZnO nanoparticles. The band gap narrowing was observed due to merging of an impurity band into the conduction band, thereby shrinking the band gap. Formation of such impurity band giving rise to new donor electronic states just below the conduction band was possible and this arises due to hybridization between states of the ZnO matrix and that of the dopants [16].

Conclusion

ZnO nanoparticles were prepared from Zinc acetate and Sodium hydroxide by precipitation method and the solution was characterized by UV-visible spectrophotometer. The nanoparticles exhibited maximum absorbance at 380 nm and its optical band gap energy was \approx 3.263eV that was narrower

than the band gap of bulk ZnO powder (3.37 eV). The resulted difference in band gap energy shows the prepared ZnO was nanoparticles. As particle size decrease the absorption edge shifts to lower wavelength or higher band gap energy. As the dopants ionic size increases, the band gap energy of ZnO nanoparticles also increases, because of the lowering of oxygen vacancy. From the studied dopants 0.015 M Li⁺ doped ZnO nanoparticles were influenced (more narrowed) the band gap energy of undoped ZnO nanoparticles than Na⁺ and K⁺ doped ZnO nanoparticles.

Acknowledgement

We thankfully acknowledge the Department of Chemistry, College of Natural Sciences, Jimma University, Jimma, Ethiopia for providing necessary facilities to carry out this work.

References

- [1]. Pan, Z. W.; Dai, Z. R.; Wang, Z. L., Nanobelts of semiconducting oxides. *Science* 291 (2001), 1947-1949.
- [2]. Özgür, Ü. A. Y. I.; Liu, C.; Teke, A.; Reshchikov, M. A.; Doğan, S.; Avrutin, V.; Cho, S. J.; Morkoc, H. A., Comprehensive review of ZnO materials and devices. *J. Appl. Phys.* 98 (2005) 041301.
- [3]. Moezzi, A.; Mcdonagh. A. M.; Cortie. M. B., Review: Zinc oxide particles: synthesis, properties and applications. *J. Chem. Eng.* 1 (2012) 185-186.
- [4]. Shanmuganathan, G.; Banu, I. S., Studies on the optical constants of K and Fe codoped ZnO thin films prepared by chemical bath deposition. *Innov. Res. Sci. Technol.* 4 (2000) 5.
- [5]. Chawla, S.; Jayanthi, K.; Kotnala, R. K., Room-temperature ferromagnetism in Li⁺ doped P-type luminescent ZnO nanorods. *Phys. Rev. B* 79 (2009) 125-204.
- [6]. Wei, S. H.; Zhang, S. B., Chemical trends of defect formation and doping limit in II-VI semiconductors. *Phys. Rev. B*, 66 (2002) 073202.
- [7]. Lim, K. H.; Kim, S.; Park, S. Y.; Kim, H.; Kim, Y. S., UV-visible spectroscopic analysis of electrical properties in alkali metal-doped amorphous zinc tin oxide thin-film transistors. *Adv. Mater.* 25 (2013) 2994-3000.
- [8]. Yu, J.; Yu, X., hydrothermal synthesis and photocatalytic activities of ZnO hollow spheres. *Environ. Sci. Technol.* 42 (2008) 4902-4907.
- [9]. Tauc, J., Amorphous and liquid semiconductors. Plenum Press, New York, 1974, 1, 171.
- [10]. Pesika, N.S. S.; Searson, K. J., Determination of the particle size distribution of quantum nanocrystals from absorbance spectra. *Adv. Matter*, 15 (2003) 1289-1291
- [11]. Changiz, V. A. E., Quantum size effects on effective mass and band gap of semiconductor quantum dots. *Res. J. Recent Sci.* 2 (2013) 21-24.
- [12]. Sunil, C. M. K.; Sandeep, C.; Katyal, S. C.; Awana, V. P. S., Structural, vibrational, optical and magnetic properties of sol-gel derived Nd-doped ZnO nanoparticles. *J. Mater. Sci. Mater. Electron.* 24 (2013) 5102-5110
- [13]. Maa, Q. Z. Y.; Zhang, A.; Lu, M.; Zhou, G.; Li, C., Synthesis and optical properties of novel red phosphors YNbTiO₆:Eu³⁺ with highly enhanced brightness by Li⁺ doping. *Solid State Sci.* 11 (2009) 1124-1130.
- [14]. Li, H. H. Y.; Li, Z.; Yao, Y.; Zhang, S., Preparation and infrared emissivities of alkali metal doped ZnO powders. *J. Cent. South Univ.* 21 (2014) 3449-3455.
- [15]. Mondal, S. B. S. R.; Mitra, P., Effect of Al doping on microstructure and optical band gap of ZnO thin film synthesized by successive ion layer adsorption and reaction. *J. Phys.* 80 (2013) 315-326.
- [16]. Park, S.Y.; Kim, K.; Lim, K.H.; Kim, B. J.; Lee, J. H. C.; Kim, S.Y., The structural, optical and electrical characterization of high performance, low temperature and solution processed alkali metal doped. *J. Mater. Chem. C*, 1(2013) 1383-1391.